Sensitivity of the Carbon Storage of Potential Vegetation to Historical Climate Variability and CO_2 in Continental China

MAO Jiafu[*1] (毛嘉富), WANG Bin[1] (王 斌), and DAI Yongjiu[2] (戴永久)

[1]*State Key Laboratory of Numerical Modeling for Atmospheric Sciences and Geophysical Fluid Dynamics (LASG),*

Institute of Atmospheric Physics, Chinese Academy of Sciences, Beijing 100029

[2]*School of Geography, Beijing Normal University, Beijing* 100875

ABSTRACT

The interest in the national levels of the terrestrial carbon sink and its spatial and temporal variability with the climate and CO_2 concentrations has been increasing. How the climate and the increasing atmospheric CO_2 concentrations in the last century affect the carbon storage in continental China was investigated in this study by using the Modified Sheffield Dynamic Global Vegetation Model (M-SDGVM). The estimates of the M-SDGVM indicated that during the past 100 years a combination of increasing CO_2 with historical temperature and precipitation variability in continental China have caused the total vegetation carbon storage to increase by 2.04 Pg C, with 2.07 Pg C gained in the vegetation biomass but 0.03 Pg C lost from the organic soil carbon matter. The increasing CO_2 concentration in the 20th century is primarily responsible for the increase of the total potential vegetation carbon. These factorial experiments show that temperature variability alone decreases the total carbon storage by 1.36 Pg C and precipitation variability alone causes a loss of 1.99 Pg C. The effect of the increasing CO_2 concentration alone increased the total carbon storage in the potential vegetation of China by 3.22 Pg C over the past 100 years. With the changing of the climate, the CO_2 fertilization on China's ecosystems is the result of the enhanced net biome production (NBP), which is caused by a greater stimulation of the gross primary production (GPP) than the total soil-vegetation respiration. Our study also shows notable interannual and decadal variations in the net carbon exchange between the atmosphere and terrestrial ecosystems in China due to the historical climate variability.

Key words: dynamic global vegetation models, China, terrestrial carbon storage, climate-vegetation interaction, CO_2 fertilization

Citation: Mao, J. F., B. Wang, and Y. J. Dai, 2009: Sensitivity of the carbon storage of potential vegetation to historical climate variability and CO_2 in continental China. *Adv. Atmos. Sci.*, **26**(1), 87–100, doi: 10.1007/s00376-009-0087-z.

1. Introduction

The terrestrial ecosystem and the climate system are closely coupled and the response of ecosystem processes at different scales to climate change, resulting from human activities, has concentrated the minds of climatologists and ecologists (Woodward et al., 2001; Cao et al., 2003). It has been suggested that the interaction between terrestrial ecosystems and the atmosphere is sensitive to changes in the climate and in atmospheric carbon dioxide concentrations; this interaction may render terrestrial ecosystems as important carbon sinks (Dai and Fung, 1993; Melillo et al., 1996; Tian et al., 1999; Woodward, 2002). The effect of the historical atmospheric CO_2 concentration and climate change on the terrestrial carbon storage, however, cannot be observed directly at regional or global scales (Grace et al., 1995; Cramer et al., 2001). The land ecosystem model (correlative or process-based model) is developed based on extensively con-

firmed eco-physiological, biophysical, and biogeochemical mechanisms, and is driven with actual changes in environmental conditions and ecosystem patterns (such as climate, vegetation, soil and human activity) (Shugart, 1998; Cao et al., 2003; Woodward and Lomas, 2004). It, therefore, has a great potential to capture the land ecosystem state pattern at different time and spatial scales. Dynamic global vegetation models (DGVMs) (Foley et al., 1996; Cramer et al., 2001; Sitch et al., 2003; Woodward and Lomas, 2004) belong to a new generation of process-based land ecosystem models, which have the potential for coupling fluxes of mass and momentum to general circulation models of the climate (Cox et al., 2000; Bonan et al., 2003) and providing a potentially more realistic simulation of the vegetation at regional and global scales in a future uncharted climate. In this study, we attempt to establish a basic understanding of processes controlling the carbon storage change in natural terrestrial ecosystems. We use the M-SDGVM (Woodward et al., 1995; Woodward and Lomas, 2004; Mao, 2006), a modified version of the Sheffield Dynamic Global Vegetation Model (SDGVM) in Woodward and Lomas (2004), to investigate the dynamics of terrestrial carbon fluxes and storage in potential vegetation of China during the last century. We focus on continental China for 3 reasons: (1) High uncertainties in estimating the national terrestrial carbon sink levels and their spatial and temporal variability with climate; the CO_2 concentrations and the debate about how to implement the Kyoto Protocol (IGBP Terrestrial Carbon Working Group, 1998); (2) China has the third largest land area with diverse climates and biomes. The climatic variability, topographic complexity, natural ecosystem diversity, as well as the human disturbance give China

Fig. 1. Comparison between the estimated NPP (g C m^{-2} yr^{-1}) with M-SDGVM and that from the Global Primary Production Data Initiative (GPPDI). The thick line is the 1 to 1 line and the filamentary line is the linear fit between the model and observations.

an important role in and large contribution to the global carbon cycle (Fang et al., 1996a,b; Ni, 2001; Cao et al., 2003; Liu et al., 2005; Lü et al., 2006); (3) The former simulations on the responses of China to climate change and the atmospheric CO_2 concentrations mainly focused on the equilibrium responses using empirical, biogeographical, or biogeochemical models (Zhou and Zhang, 1996; Xiao et al., 1998; Yang et al., 2001; Ni, 2001, 2002; Cao et al., 2003; Tao, 2003; Fang et al., 2003; Huang, 2005). In this paper, we use the M-SDGVM to study the transient responses of the Chinese terrestrial ecosystem structure, composition, and carbon storage on vegetation and soil to changes in climate and the atmospheric CO_2 concentrations from 1901 to 2000.

2. Materials and methods

2.1 *Model description*

DGVMs are designed to simulate vegetation responses to changing climates. They simulate carbon and water dynamics and the vegetation structure by using input data of the climate, soil properties, and the atmospheric CO_2 concentrations in an integrated system (Woodward et al., 1995; Foley et al., 1996; Beerling and Woodward, 2001; Cramer et al., 2001). The models generate predictions of the composition and structure of vegetation for a given climate in terms of relatively few plant functional types (PFTs, e.g., Woodward et al., 1995; Haxeltine and Prentice, 1996; Bonan et al., 2002a). The standard SDGVM (Woodward et al., 1995; Woodward and Lomas, 2004) is one kind of DGVMs that predicts the global-scale vegetation structure and dynamics from input data such as climate, CO_2, and soil texture (Fig. 1 in Mao et al., 2007). The physiology and biophysical module simulates carbon and water fluxes from vegetation (Woodward et al., 1995) with water and nutrient supply defined by the water and nutrient flux module. The soil module incorporates the soil carbon and nitrogen dynamics of century ecosystem model (Parton et al., 1993) with a model of plant water uptake. Soil water fluxes are modeled using a "bucket" model with four buckets: one thin (5 cm) layer at the surface and three buckets of equal depths, which make up the remainder of the soil layer. The effects of bare soil evaporation, snow sublimation, vegetation transpiration, and canopy interception (each of which represents a loss of water available to the vegetation system) are incorporated into the model. The primary productivity model simulates the canopy CO_2, the water vapor exchange, nitrogen uptake, and partitioning within the canopy. The plant structure and phenology module defines the vegetation leaf area index and the vegetation phenol-
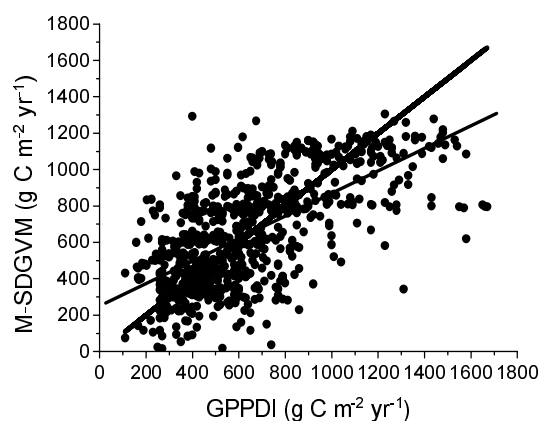
ogy. To account for the establishment, growth, competition, and mortality among plants in the vegetation dynamics module, 8 plant functional types (Table 1) are distinguished. The fire module, based on temperature and precipitation, burns a small fraction of the pixel and it will be called at a random time and for a random subset of the pixel at a critical point of dryness. After evaluations and calibrations of the carbon and water budgets of the standard SDGVM with site-specific measurements, inventory data, and model outputs in China, one updated version, fit for the Chinese terrestrial ecosystems, named "Modified Sheffield Dynamic Global Vegetation Model (M-SDGVM)" (Mao, 2006; Mao et al., 2007) was established and used in this paper. Compared with the standard version described above, the M-SDGVM has some new parameterization schemes including the incorporation of numerical processes related to radiation, root profiles, and soil physical characters, and the adoption of a higher resolution vegetation map, and a soil texture dataset of China. A few of the PFTs specific parameters had to be re-adjusted to ensure realistic simulations of the carbon and water balance after these modifications. A detailed description of parameterizations is described in detail in Mao (2006) and Mao et al. (2007).

2.2 *Evaluations of M-SDGVM*

Evaluations of the reliability of the M-SDGVM on China are appropriate before the factorial experiments. After setting up the updated M-SDGVM, we calibrated it with the field-derived net ecosystem production (NEP) and evapotranspiration (EVT) measured around the globe using the eddy covariance technique. 15 EUROFLUX sites (Valentini, 2002; Mao, 2006) including the upland oak forest on the Walker Branch Watershed in Tennessee (Hanson et al., 2004; Mao et al., 2007) and sites of the Chinese forest and grassland (Liu et al., 2004), have been employed to evaluate the model's carbon and water cycles at different time scales. Evaluations and calibrations of the M-SDGVM using eddy covariance data showed that the model performed well on simulating the carbon and water fluxes of different ecosystem types under different climate conditions. Besides validations with the eddy covariance-based measurements at the grid cells, some of the best regional datasets such as the forest inventory-based NPP measurements and the models output of the Chinese soil-vegetation system were also used for tests. The modeled contemporary NPP of the major Chinese forest types, including 743 study sites from 7 PFTs in China, fit satisfactory with the NPP included in the Global Primary Production Data Initiative (GPPDI) data set (Prince et al., 1995; Olson et al., 2001a) obtained from published forest reports, as well as from Chinese journals and some unpublished literature (Luo, 1996; Ni, 2001; Dan et al., 2005; Mao, 2006). Figure 1 shows the comparison between the NPP estimation with M-SDGVM and GPPDI measurements. Compared to the observations, although there is a systemic underestimation of NPP, which may probably attribute to the model's low estimation of GPP, the M-SDGVM demonstrates a good performance on China's main ecosystem types ($R = 0.66, P < 0.0001$) in different climate regions. The average NPP simulated by the M-SDGVM from 1981 to 2000 in China is 3.299 Pg C yr^{-1}, which is consistent with other earlier model outputs for the same time period (3.653 Pg C yr^{-1}, Xiao et al., 1998; 3.09 Pg C yr^{-1}, Tao, 2003; 3.445 Pg C yr^{-1}, Huang, 2005). Other simulations of the soil-vegetation carbon storage and fluxes in China, including the vegetation-soil carbon density, soil moisture, heterotrophic respiration (RH), and the leaf area index (LAI) were also evaluated in detail in Mao (Mao, 2006).

2.3 *Data sources*

Considering the cost of the model integration, we ran the M-SDGVM with observation-based climate data, atmospheric CO_2, and vegetation distribution at a spatial resolution of 0.5° and a time-step of one day. The climate data was derived from the Climate Research Unit's (CRU TS 2.1) 20th century climate monthly data set (1901–2000, Mitchell and Jones, 2005) that were used to create daily data and the time resolution of the model by a simple weather generator in the M-SDGVM. A data set of the historical global atmospheric CO_2 concentrations extending from 1901 to 2000 was obtained courtesy of the Carbon Cycle Model Linkage Project (McGuire et al., 2001). The up-layer (0–30 cm) soil properties were derived from the National Soil Survey (Huang, 2005), and the down-layer (30–100 cm) textures, because of the lack of observations, were based on the hybrid soil texture of the Food and Agriculture Organization's (FAO) (Batjes et al., 1997) global soil data set and the U.S. Department of Agriculture's 16-category State Soil Geographic Database (STATSGO). Both layers were organized in a grid at 0.1° × 0.1° resolution. The Chinese land cover classification at a 0.10 grid resolution is the potential hybrid vegetation from the vegetation map of China at a 1:4000000 scale (Hou, 1983); the Global Vegetation Monitoring Unit (GVM) represents an improvement over the global classification schemes available from sensors such as the Moderate-resolution Imaging Spectroradiometer (MODIS). The combined vegetation classification scheme comprises 19 cover types, which have been regrouped into 8 plant functional types for this study (Table 1). At the begin-

ning of each year's run of the M-SDGVM, a fraction of the ground becomes available for new growth and the land cover defined in the M-SDGVM input file determines how this new ground is to be allocated between the PFTs.

2.4 Experimental design

The M-SDGVM simulations start from a soil, defined by texture, depth, climate, and atmospheric CO_2 concentration. Therefore, there is a necessary initialization stage in which the carbon and nitrogen storage of the soil is determined using the appropriate vegetation for the simulated climate. The model initialization is determined by running with a repeated and random selection of annual climates from 1901 to 1920. The soil's carbon and nitrogen values are first determined by solving century ecosystem model analytically (Parton et al., 1993). The model then runs until the vegetation structure is at equilibrium, typically after, at most 600 years. When the initialization is completed, the M-SDGVM then simulates the vegetation for the whole climate series. In this paper, we designed a series of five experiments (Table 2) to examine the sensitivity of terrestrial carbon fluxes and storage in China to historical atmospheric CO_2 concentrations, air temperatures, and precipitation during the 20th century. In Expt. 1, the atmospheric CO_2 concentrations between 1901 and 2000 were used as inputs

to the M-SDGVM to examine the effects of increasing CO_2 on terrestrial carbon fluxes and pools. In this experiment, we used the monthly mean temperature and precipitation data from 1901 to 1930, generated from the gridded data sets described above. In Expt. 2, the historical temperatures between 1901 and 2000 were used as inputs to examine the effects of temperature variability on terrestrial carbon fluxes and pools. This experiment also used the constant atmospheric CO_2 concentration in 1901 (296.3 ppmv) throughout the simulation period and the long-term monthly mean precipitation data from 1901 to 1930, generated from the gridded historical precipitation data set described above. In Expt. 3, the historical precipitation between 1901 and 2000 were used as inputs to examine the effects of precipitation variability on terrestrial carbon fluxes and pools. This experiment also used a constant atmospheric CO_2 concentration of 296.3 ppmv throughout the study period and the long-term monthly mean temperature data from 1901 to 1930. In Expt. 4, the historical temperatures and precipitation between 1901 and 2000 were used as M-SDGVM inputs to examine the effects of temperature and precipitation variability on terrestrial carbon fluxes and pools. The CO_2 concentration was also kept a constant 296.3 ppmv throughout the study period. In Expt. 5, we used the historical CO_2 concentrations of Expt. 1, historical temperature data of Expt. 2, and historical

Table 1. The hybrid vegetation map and PFTs equivalents in the M-SDGVM simulations.

Hybrid vegetation map number	Land cover types	Percent of M-SDGVM PFTs
1	"Evergreen Needleleaf Forest"	100% Ev_Nl
2	"Evergreen Broadleaf Forest"	100% Ev_Bl
3	"Deciduous Needleleaf Forest"	100% Dc_Nl
4	"Deciduous Broadleaf Forest"	100% Dc_Bl
5	"Mixed Forest"	50% Dc_Bl 50% Ev_Nl
6	"Closed Shrublands"	100% C3
7	"Open Shrublands"	100% C3
8	"Woody Savannas"	30% C3 70% Dc_Bl
9	"Savannas"	50% C3 50% Dc_Bl
10	"Grasslands"	100% C3
11	"Permanent Wetlands"	100% C4
12	"Cropland in the South"	100% Crop
13	"Cropland in the North"	100% Crop
14	"Cropland/nature vegetation mosaic"	30% Dc_Bl 30% C3 40% Crop
15	"Desert Steppe"	100% C3
16	"Barren or Sparsely vegetated"	50% C3 50% BARE
17	"Urban"	100% BARE
18	"Snow and Ice"	100% BARE
19	"Water body"	100% BARE

Notes: Ev_Bl, Ev_Nl, Dc_Bl and Dc_Nl represent evergreen broadleaved trees, evergreen needleleaved trees, deciduous broadleaved trees, and deciduous needleleaved trees respectively. C3, C4, Crop and BARE represent grass with C3 or C4 photosynthetic path, cropland, and bare ground functional types.

Table 2. Experiment designs.

Expt.	CO$_2$	Temperature	Precipitation	Other forcing data sets
1	Historical	Monthly mean	Monthly mean	Historical
2	296.3 ppmv	Historical	Monthly mean	Historical
3	296.3 ppmv	Monthly mean	Historical	Historical
4	296.3 ppmv	Historical	Historical	Historical
5	Historical	Historical	Historical	Historical

Table 3. Responses and linear fit (Pg C yr^{-1}) of vegetation carbon, soil carbon, total carbon storage (Pg C) to changes in atmospheric CO$_2$ and climate variability in continental China during from 1901–2000 for different experiments.

Expt.	Vegetation carbon			Soil carbon			Total carbon		
	Increase of carbon (Pg C)	Increase rate compared to the baseline (%)	Linear fit of carbon increase (Pg C yr^{-1})	Increase of carbon (Pg C)	Increase rate compared to the baseline (%)	Linear fit of carbon increase (Pg C yr^{-1})	Increase carbon of (Pg C)	Increase rate compared to the baseline (%)	Linear fit of carbon increase (Pg C yr^{-1})
1	2.19	+15.3	0.02	1.03	1.1	0.02	3.22	2.9	0.02
2	−0.04	−0.3	−0.0005	−1.32	−1.4	−0.01	−1.36	−1.2	−0.02
3	−0.07	−0.5	−0.002	−1.92	−2.0	−0.02	−1.99	−1.8	−0.03
4	−0.05	−0.3	−0.001	−2.08	−2.2	−0.02	−2.13	−1.9	−0.03
5	2.07	14.48	0.02	−0.03	−0.03	−0.01	2.04	1.9	0.01
1+2+3	2.08	14.55		−2.21	−2.3		−0.13	−0.1	
5−(1+2+3)	−0.01	−0.07		2.18	2.3		2.17	2.0	

precipitation data of Expt. 3 to examine the combined effects of increasing atmospheric CO$_2$ concentrations and the climate variability on carbon fluxes and pools. For all five experiments we adopted the same historical humidity and cloud data sets described above between 1901 and 2000.

3. Results

3.1 Transient effect of CO$_2$ fertilization

Based on the M-SDGVM initialization for different experiments, we indicate that for potential vegetation before 1900 in continental China, the baseline of the vegetation carbon pool is 14.3 Pg C, the soil carbon pool is 95.1 Pg C, and the total carbon storage is 109.4 Pg C (Table 3). In response to the historical atmospheric CO$_2$ concentration alone (Expt. 1) (Fig. 2a), the M-SDGVM simulation shows that during the last 100 years, the total carbon pool increases at a rate of 0.02 Pg C yr^{-1}; 0.02 Pg C yr^{-1} for the vegetation carbon pool, and 0.01 Pg C yr^{-1} for the soil carbon pool (Table 3). The total carbon storage in the potential vegetation of China increases by 3.22 Pg C (2.9%) over the past 100 years, with 2.19 Pg C (15.3%) stored in vegetation and 1.03 Pg C (1.1%) stored in organic soil matter (Fig. 2b, Table 3). The continuous increase in the carbon storage in potential vegetation and soil in China between 1901 and 2000 is a consequence of the continuous increase of the net biome production (Fig. 2c), the difference of NPP, RH (Fig. 2d) and the carbon released by disturbances like fires. The maximum carbon source (−0.24 Pg C) during the 100 years can be seen in 1954, but the maximum carbon sink (0.39 Pg C) occurs in 1986 (Fig. 2c). NBP shows a continuous increase over time from −0.07 Pg C (minus represents the release of carbon from the terrestrial ecosystem to the atmosphere) in 1901 to 0.15 Pg C in 2000, with an average increase of 0.002 Pg C per year (Fig. 2c). Thus, relatively more carbon is stored in terrestrial ecosystems each year as CO$_2$ concentrations increase.

3.2 Transient effect of temperature variability

Based on the M-SDGVM simulations, we conclude that temperature variability alone (Expt. 2) has not induced an evident change in the total carbon storage for potential vegetation in continental China over the past 100 years. Most PFTs showed a decrease in the total carbon storage, but the range in PFTs response was quite small (figure omitted). Carbon storage in different PFTs has different responses over the simulation period because of different sensitivities to the changes of temperature and because of different spatial variations in the temporal patterns of temperature
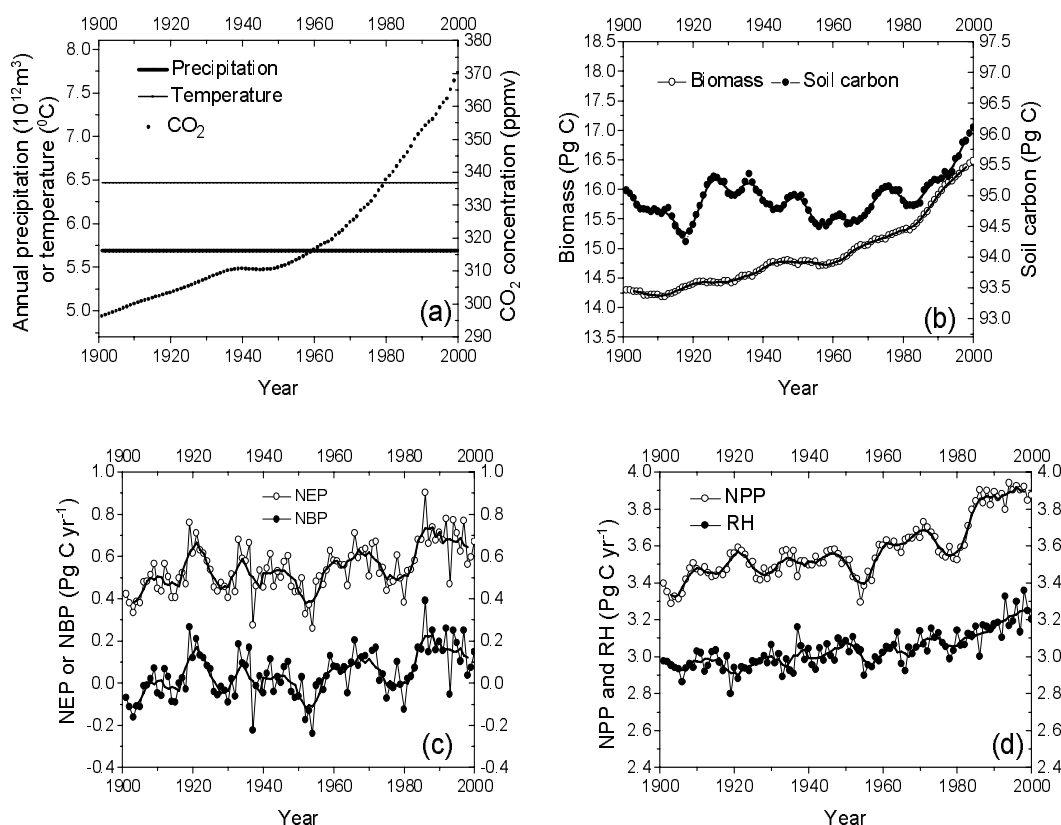
Fig. 2. (a) Interannual variations in air forcing, (b) total biomass and the organic soil carbon pool, (c) net ecosystem production (NEP), net biome production (NBP), (d) net primary production (NPP), and heterotrophic respiration (RH) in continental China induced by historical CO_2 concentrations alone from 1901–2000. The thick line is 5-year annual mean.

(figure omitted) (Tian et al., 1999; McGuire et al., 2001). The total carbon storage decreased by 1.36 Pg C (-1.2%; -0.02 Pg C yr^{-1}), with 0.04 Pg C (-0.3%; -0.0005 Pg C yr^{-1}) lost in vegetation and 1.32 Pg C lost (-1.4%; -0.01 Pg C yr^{-1}) from the organic soil carbon (Fig. 3b, Table 3). The interannual patterns of the net ecosystem production, NBP, NPP, and RH show notable year-to-year fluctuations (Figs. 3c, d), which are associated with interannual and decadal variations of the temperature during the 20th century (Fig. 3a). In response to the variation of temperature, the balance between NPP, RH, and disturbances cause periods when the terrestrial ecosystems of China are sources of atmospheric carbon (i.e., negative NBP) and other periods when these ecosystems are carbon sinks (i.e., positive NBP) (Fig. 3c).

3.3 Transient effect of precipitation variability

In response to historical precipitation variability alone (Expt. 3), the M-SDGVM simulation indicates that the total carbon storage decreased by 1.99 Pg C (-1.8%; -0.03 Pg C yr^{-1}), with 0.07 Pg C (-0.5%;

-0.002 Pg C yr^{-1}) lost in vegetation and 1.92 Pg C (-2.0%; -0.02 Pg C yr^{-1}) lost from the organic soil carbon (Fig. 4b, Table 3). Like the temperature variations only, different responses of the carbon storage in different PFTs (figure omitted) over the simulation period are the result of different sensitivities to changes in precipitation as well as spatial variations in the temporal patterns of precipitation (figure omitted). From 1901 and 2000, terrestrial ecosystems in China experienced evident variability in precipitation (Fig. 4a). For potential vegetation of China, increases (or decreases) in precipitation tend to increase (or decrease) NEP, NBP, NPP, and RH (Figs. 4a–d). Evident decreases in precipitation occurred in the 1920s, the mid 1930s to the mid 1940s, and the mid 1970s to the first part of the 1980s, are accompanied by a minus NBP, a source of atmospheric CO_2 from terrestrial ecosystems. In contrast, during wet years, such as the mid 1980s to the first part of the 1990s, terrestrial ecosystems are sinks of atmospheric CO_2 (Fig. 4c). As a result of the interannual precipitation variability, the net carbon flux estimated by the M-SDGVM for the potential vegetation in China during the 20th century
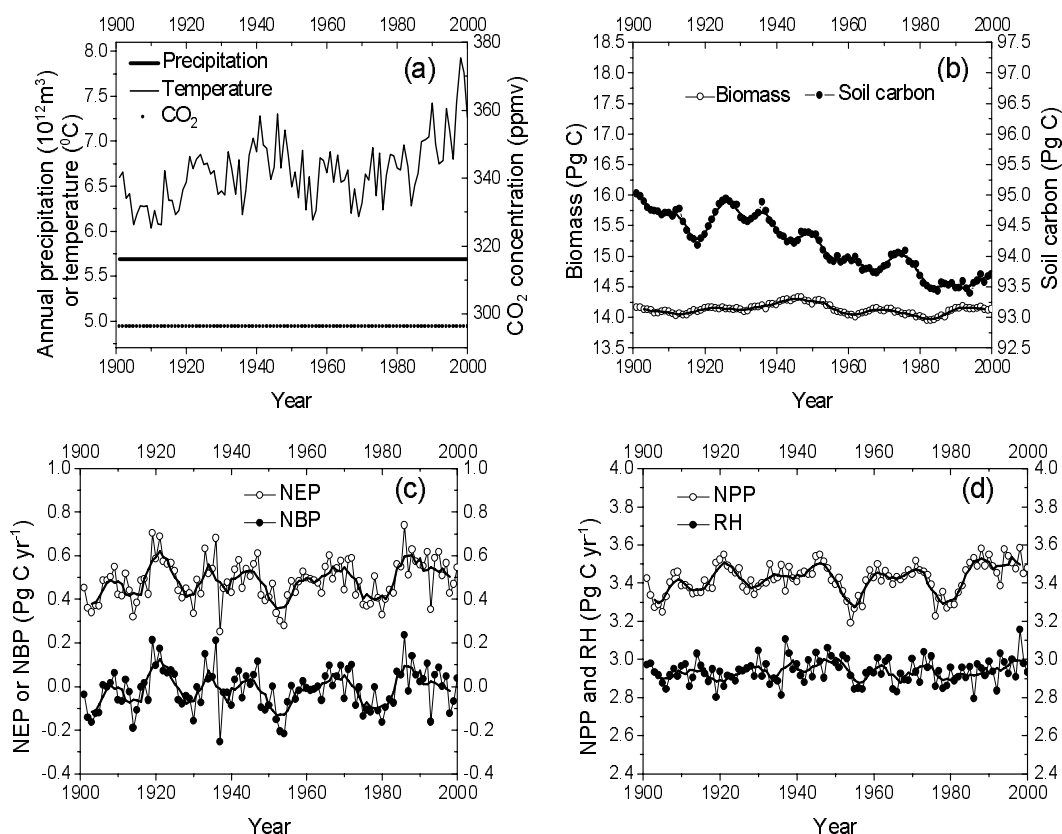
Fig. 3. As in Fig. 2, but induced by historical temperatures alone from 1901–2000.

varied from a maximum source of atmospheric CO_2 (-0.31 Pg C) in 1937 to a maximum sink of atmospheric CO_2 (0.24 Pg C) in 1992 (Fig. 4c). The increasing precipitation (a slope of 1.3×10^9 m^3 per year) during the last century (Fig. 4a) leads to an increasing soil moisture and RH (Fig. 4d), and as a result, the evident decreasing of the soil carbon pool compared with the variation of the vegetation biomass (Fig. 4b, Table 3). The soil-vegetation EVT can influence canopy conductance, canopy intercellular CO_2, and the water on leaves which can reduce the area for transpiration (Sellers et al., 1986; Dai et al., 2003), and as a result, plays an important role in the vegetation GPP and NPP. The response of NPP to the interannual variation of precipitation is very tightly coupled with the total EVT ($R=0.6$, $N=100$, $P < 0.0001$), and moderately coupled with the organic soil carbon and nitrogen pool (figure omitted).

3.4 *Transient effect of climate variability*

In response to a combination of the historical temperature and precipitation variation (Expt. 4) (Fig. 5a), we show that the total carbon storage, the vegetation carbon in biomass, and the organic soil carbon (Fig. 5b) are similar to the response of the carbon storage to the precipitation variation alone from 1901 to 2000 in China (Fig. 4b). The total carbon storage, however, decreased by 2.13 Pg C (-1.9%; -0.03 Pg C yr^{-1}), with 0.05 Pg C (-0.3%; -0.001 Pg C yr^{-1}) in vegetation biomass and 2.08 Pg C (-2.2%; -0.02 Pg C yr^{-1}) in the organic soil carbon matter (Table 3). Because the simulated NEP, NBP, NPP, and RH (Figs. 5c, d) are more sensitive to the variation of precipitation than to the variation of temperature, the interannual patterns of them for the combination of the historical temperature and precipitation variations are more like the patterns for the precipitation variation alone.

3.5 *Transient effect of climate variability and increasing* CO_2 *concentration*

In response to a combination of climate variability and increasing CO_2 concentrations (Expt. 5), the M-SDGVM estimated that during the 20th in China the total vegetation carbon storage in the potential vegetation increased by 2.04 Pg C (1.9%; 0.01 Pg C yr^{-1}), with 2.07 Pg C (14.5%; 0.02 Pg C yr^{-1}) gained in vegetation biomass and 0.03 Pg C (-0.03%; -0.01 Pg C yr^{-1}) lost from organic soil carbon matter (Fig. 6b,
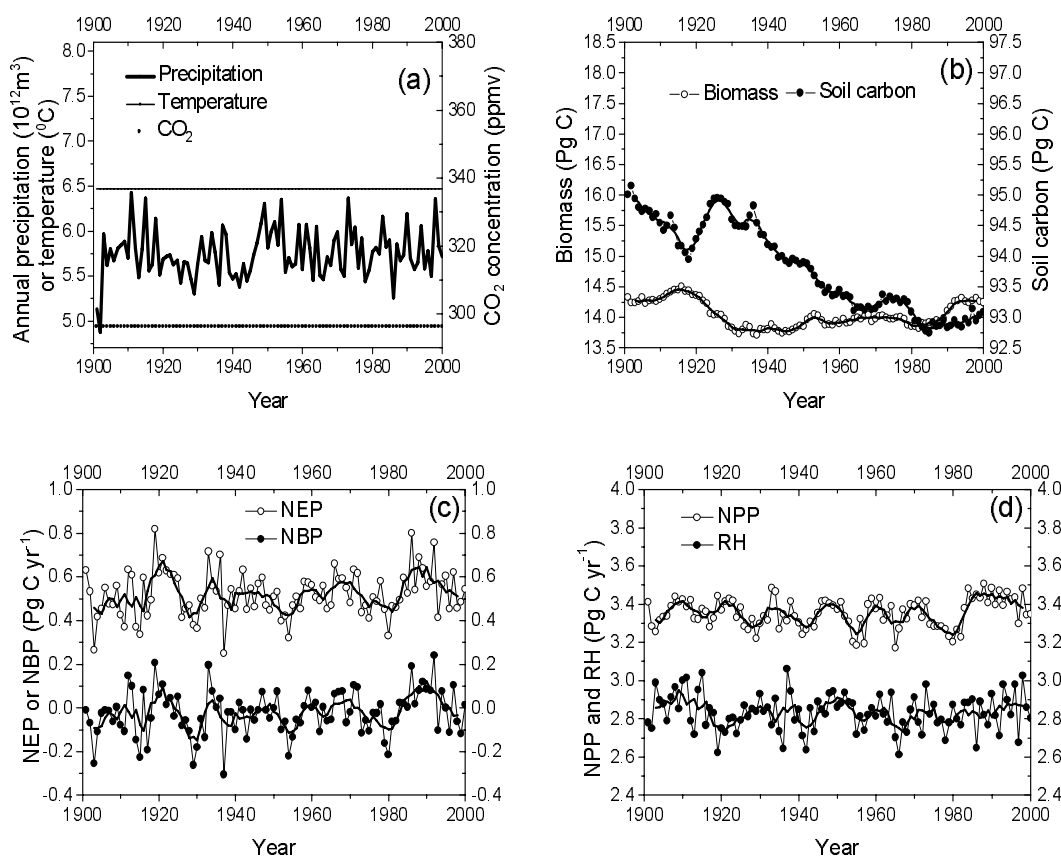
Fig. 4. As in Fig. 2, but induced by the historical precipitation alone from 1901–2000.

Table 3). Our factorial experiments show that increasing CO_2 concentrations over the past 100 years was primarily responsible for the increase of the total potential vegetation carbon. For the increasing tendency of the biomass carbon, organic soil carbon, NEP, NBP, NPP, and RH (Figs. 6b–d), they are similar to those in experiment 1, where only CO_2 changes with time (Figs. 2b–d). The interannual variation patterns of the NEP, NBP (Fig. 6c), NPP, and RH (Fig. 6d) are very similar to those in experiment 3, where only precipitation was allowed to change over the study period (Figs. 4c–d). Thus, in the combined experiment, the precipitation explains most of the interannual variation in the net carbon exchange (NBP) between the atmosphere and the terrestrial ecosystems, with a maximum carbon release of 0.27 Pg C in 1937 and a maximum carbon uptake of 0.36 Pg C in 1992 (Fig. 6c). Totally, in the interactions among CO_2, temperature and precipitation along with the effects of CO_2, fertilization outpaces the climate-induced carbon losses. The M-SDGVM simulations of the terrestrial ecosystems in continental China tend to be a sink of atmospheric CO_2 with an average of 0.032 Pg C yr^{-1} during the last century. However, the overall response of vegetation, soil, and the total carbon storage to a com-

bination of climate variability and the increasing CO_2 is not completely explained by simply adding together the individual responses affected by CO_2 fertilization, temperature, and precipitation variations (Table 3). The CO_2 fertilization alone in experiment 1 did not compensate for the individual effect of the temperature and precipitation induced carbon loss; there was 0.13 Pg C (-0.1%) lost in the total carbon, 2.08 Pg C (14.55%) gain in the vegetation carbon, and 2.21 Pg C (-2.3%) lost in the soil carbon pool (Table 3). As a result, the transient interactions among the climate variability and CO_2 concentrations accounted for an additional 2.17 Pg C (2.0%) in the carbon storage, with 0.01 Pg C (-0.07%) lost from the vegetation carbon and 2.18 Pg C (2.3%) stored in the soils (Table 3).

3.6 *The effect of* CO_2 *fertilization under the historical climate change on the ecosystems of continental China*

Comparing Expt. 5 with Expt. 4, we changed the constant CO_2 to vary with time and as a result, the variation caused by the CO_2 fertilization under the same climate background can be isolated. Expt. 5 showed that the CO_2 fertilization could play a very important role on the sink of terrestrial ecosystems in
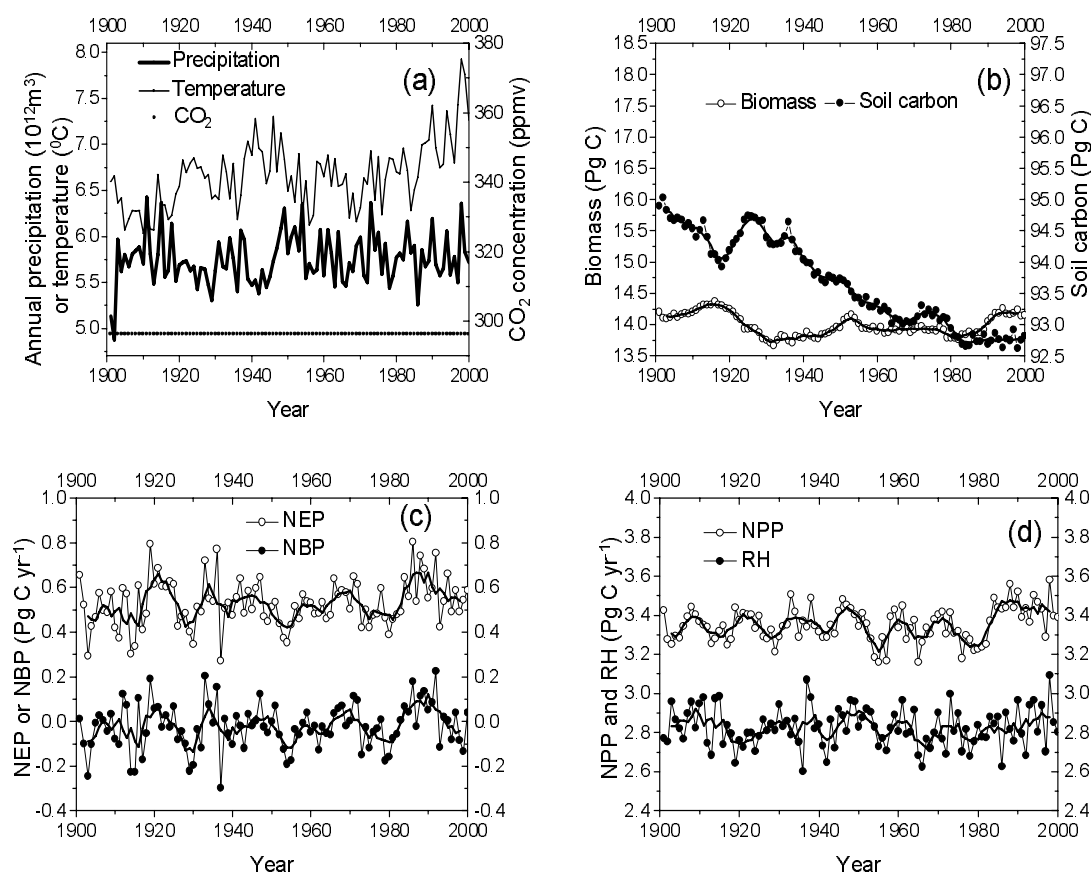
Fig. 5. As in Fig. 2, but induced by the historical climate from 1901–2000.

continental China. The simulations during the 20th century, indicated a clear CO_2 fertilization (Figs. 7a–c) effect on the terrestrial sink in continental China, with particularly notable differences from the 1980s, a period coinciding with more rapid increases in temperature and CO_2 concentrations (Fig. 6a). The enhanced NBP under the increasing CO_2 scenario is caused by a greater stimulation of GPP than the total vegetation respiration (Fig. 7a). The CO_2 stimulation increases with CO_2 concentrations and also with the warmer climate of the 1980s and 1990s (Fig. 6a), which exerts a stronger positive impact on the GPP than on vegetation respiration (Fig. 7a). The majority of the changes in carbon sequestration by vegetation are due to the changes in biomass, which is simulated to have increased more or less monotonically from the 1940s alongside increasing CO_2 concentrations (Fig. 7b). A similar result can be seen in the global simulation with the standard SDGVM, in which the biomass also increased from the 1940s with the increasing CO_2 (Woodward and Lomas, 2004). In comparison with the change of the biomass carbon, the relative changes in soil carbon are even smaller, especially in Expt. 5 (Fig. 7b). One interesting feature is the lag in the response

of the soil carbon, compared to biomass, to ameliorating conditions in both experiments (Fig. 7b). As in Expt. 5, the minimum value of the vegetation biomass is simulated for 1930, while the minimum of the soil carbon occurs 35 years later. This reflects the time taken for the increase in litter carbon accumulation to move from the rapidly turning over pools to the longer-lived pools in the soil (Canadell et al., 1996; Woodward and Lomas, 2004). The early declines in biomass for both CO_2 treatments are due to reductions in terrestrial precipitation between the early 1910s and the late 1920s, combined with steady increases in temperature over the same period (Fig. 6a). The geographical distribution of the differences of the 20th century total carbon sinks in continental China between Expts. 5 and 4 show a quite complex pattern (Fig. 8). All the terrestrial ecosystems, except some areas on the Tibetan plateau in continental China, tend to increase their sink of atmospheric CO_2 because of the CO_2 fertilization. The ecosystems mainly with the evergreen needle leaf and broadleaf functional types in south China, like the Fujian and Yunnan provinces, have the highest carbon sinks (Fig. 8). The maximum sink capacity is more than 1750 g C m^{-2} over the 20th cen-
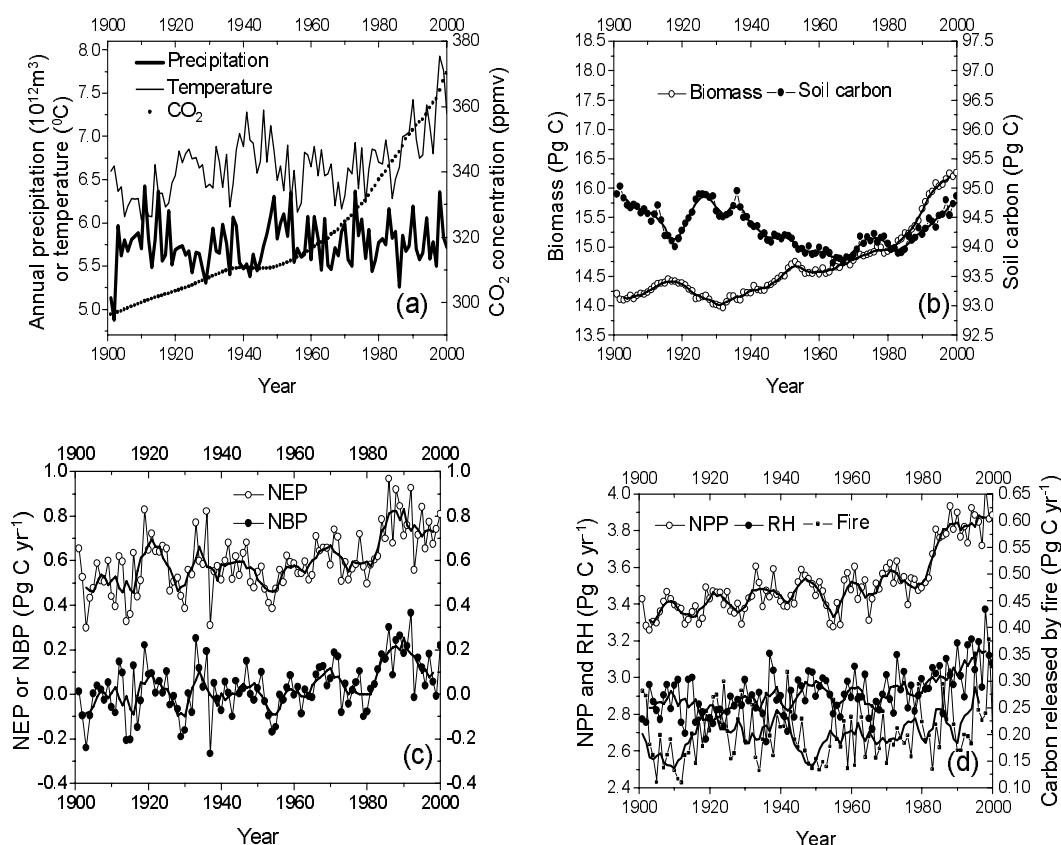
Fig. 6. (a) Interannual variations in air forcing, (b) total biomass and the organic soil carbon pool, (c) NEP, NBP, (d) NPP, RH and carbon released by fire in continental China induced by the historical climate and increasing CO_2 from 1901–2000. The thick line is 5-year annual mean.

tury, equivalent to 17.5 g C m^{-2} yr^{-1}.

4. Conclusions and discussions

In response to the historical atmospheric CO_2 concentrations alone, the M-SDGVM simulation indicates that the total carbon storage in the potential vegetation of China increases because of a continuous increase in NBP with time. It reflects that plants may increase their ability in the uptake of carbon when the atmospheric concentration of CO_2 increases. The temperature variability alone has not induced a significant change in the total carbon storage for the potential vegetation in China over the past 100 years. But with interannual and decadal variations of temperature, during the 20th century, the interannual patterns of NPP, RH, NEP, and NBP show notable year-to-year fluctuations. Like the temperature variability alone, the M-SDGVM simulation indicates that the total carbon storage in the potential vegetation in continental China only shows a little decrease in response to the historical precipitation variability alone. The increase of precipitation tends to increase NPP

and NBP, but tends to decrease the soil carbon pool as a result of the increase of soil moisture and RH. Because the simulated NPP, RH, NEP, and NBP are more sensitive to the variation of precipitation than to the variation of temperature, the interannual patterns of them in the combination of historical temperature and precipitation variations are more like the patterns for the precipitation variations alone. In response to a combination of climate variability and increasing CO_2 concentrations, the M-SDGVM estimated that during the 20th century in China, the total vegetation carbon storage in the potential vegetation increased by 2.04 Pg C and the precipitation explains most of interannual variation in the net carbon exchange between the atmosphere and the terrestrial ecosystems. The interactions among the climate variability and CO_2 concentrations in the combined experiment, however, accounted for an additional 2.17 Pg C in the carbon storage compared to the sum of the individual CO_2 concentrations, temperature, and precipitation effects. For the effect of CO_2 fertilization under the climate change on the ecosystems of China, a significant CO_2 fertilization on carbon sequestration by the terrestrial
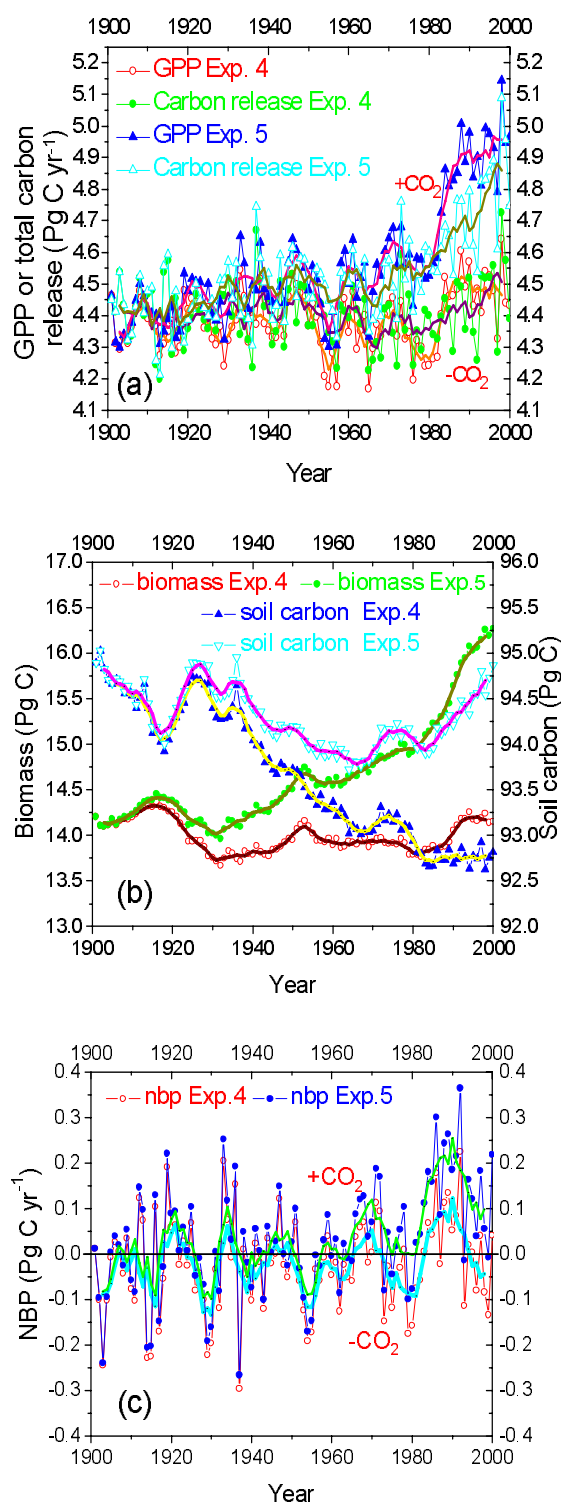
Fig. 7. Interannual variations in (a) GPP and total carbon released by respiration, (b) total biomass, the organic soil carbon pool and (c) NBP in continental China induced by the historical climate and constant CO_2 (Expt. 4; $-CO_2$), and the historical climate and increasing CO_2 (Expt. 5; $+CO_2$) from 1901–2000. The thick line is 5-year annual mean.
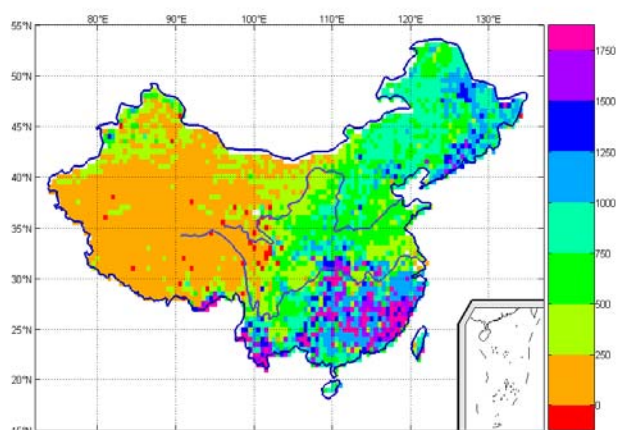

Fig. 8. Geographical distribution of the difference of the 20th century total carbon sinks (g C m^{-2}) in continental China between Expts. 5 and 4.

biosphere for most of the latitude bands of China can be found. The highest carbon sinks lie in south China, where the evergreen needle leaf and broadleaf functional types exist along with higher air temperatures and precipitation.

Solar radiation is one of the key factors constraining the vegetation photosynthesis, and the availability of solar radiation and its daily and yearly distribution has a tremendous influence on the productivity and quality of plant growth (Melillo et al., 1996; Cao et al., 2003). While in our current study, because of limitations on obtaining such long-term historical solar radiation data, calculation of the instantaneous downward shortwave radiation and net radiation was derived from Prentice et al. (1993). Consequently, trends in the carbon storage and fluxes that resulted from solar radiation cannot be fully separated from trends due to other climatic drivers. Thus, further comprehensive research of the responses of China's terrestrial ecosystem to historical solar radiation under climatic changes will aid to advance our understanding on the rules of carbon storage variations and terrestrial carbon cycles.

According to Cao et al. (2003), the warming trend stimulated vegetation growth in the northern high latitudes and increases in atmospheric CO_2 contributed to vegetation growth increases in all regions. In our simulation, compared to Expt. 4, the CO_2 fertilization (Figs. 7a–c) effect in Expt. 5 on the terrestrial sink in continental China shows notable differences especially during the rapidly warming 1980s and 1990s (Fig. 6a). This is also consistent with studies suggesting that the response of photosynthetic biochemical reactions to the increase in atmospheric CO_2 is higher under warmer conditions (Kirschbaum et al., 1994).

Nitrogen and phosphorus are the nutrients that

most often limit the productivity and functioning of terrestrial ecosystems, especially nitrogen, a primary limiting nutrient at the middle and high latitudes and an important nutrient at lower latitudes (Long et al., 2006; Wang et al., 2007). In M-SDGVM, however, the absence of phosphorus dynamics and not enough of a nitrogen deposition dataset to calibrate the nutrients' effect on the carbon dynamics in the soil module of century ecosystem model limit our analysis. In other words, on physiological grounds, the clear CO_2 fertilization in the present version of M-SDGVM may be overestimated without a nutrient constraint on the CO_2 stimulation. Hence, it is essential to include both of these element cycles in the future version of M-SDGVM. By then, there will also be a deeper understanding on the interactions between nutrient and NPP over variant time scales, which will facilitate our improvement on the systemic underestimation of NPP in Fig. 1.

We have explored how climate variability and increasing atmospheric CO_2 concentrations in the last century may have affected the carbon fluxes and storage of terrestrial ecosystems in continental China with the M-SDGVM. However, on the other hand, disturbances like fires and land use are important factors in controlling carbon sink/source behavior of the Chinese ecosystems (Ge et al., 2000; Lü et al. 2006). It is also shown in our factorial experiments that with the defaulted fire in Expt. 5, the carbon released from all terrestrial ecosystems to the atmosphere during last century in China is 0.20 Pg C per year (about 5.76 percent of the total NPP) due to the burning of the biomes (Fig. 6d). As for the land use influence, we have indicated in the introduction that China is the third largest country in land area, which has a great variability in the physical environment and has experienced notable climate variation and dramatic land transformation across the nation (Ge et al., 2000; Tian et al., 2003; Liu et al., 2005). These changes to cropland or to urbanization have important implications for the biogeochemical and hydrological cycles, including loses of soil carbon and soil phosphorus and the leaking of the soil's nitrogen. In this paper, however, we used the potential land cover of China and had not considered the responses of the vegetation distribution to climate and elevated CO_2, or the soil-vegetation carbon pool to land use/land cover change. We mainly focus on the possible influences of climate forcings and CO_2 on the regional terrestrial carbon dynamics, including fluxes and storages of carbon in continental China during the last century. We aim at finding the key factors and processes influencing the regional terrestrial carbon cycle, questing for possible feedback from the terrestrial ecosystem to the climate system

and as a result, making preparations for the instantaneous coupling between the M-SDGVM and the LASG climate system model (Yu et al., 2002). This study provides a baseline for further investigations on the impacts in land use/land cover changes on carbon fluxes and storage in China. Currently we are beginning to conduct transient simulations of the M-SDGVM, taking account of the time course of changes of land use/land cover, fire, and anthropogenic nitrogen deposition from the last several centuries to the next century. But what hinders us the most is the lack of both historical and future data with better spatial and temporal processes of climate, land use/land cover change, fire, and nitrogen deposition in continental China. As these datasets become available in the near future, we should be able to improve the estimations of the transient responses of the Chinese terrestrial ecosystems to changes in climate, atmospheric CO_2, and the disturbance regime from nature and human activity during the last century.

REFERENCES

Batjes, N. H., G. Fisher, F. O. Nachtergaele, V. S. Stolbovoy, and H. T. van Velthuizen, 1997: *Soil Data Derived from WISE for Uses in Regional and Global AEZ Studies (Version 1.0)*. FAO/IIASA/ISRIC, Laxenburg, 27pp.

Beerling, D. J., and F. I. Woodward, 2001: *Vegetation and the Terrestrial Carbon Cycle: Modelling the First 400 Million Years*. Cambridge University Press, Cambridge, UK, 405pp.

Bonan, G. B., S. Levis, L. Kergoat, and W. O. Keith, 2002a: Landscapes as patches of plant functional types: an integration concept for climate and ecosystem models. *Global Biogeochemical Cycles*, **16**, 1021–1029.

Bonan, G. B., S. Levis, S. Sitch, M. Vertenstein, and K.W. Oleson, 2003: A dynamic global vegetation model for use with climate models: concepts and description of simulated vegetation dynamics. *Global Change Biology*, **9**, 1543–1566.

Canadell, J., L. Pitelka, and J. S. Ingram, 1996: The effects of elevated CO_2 on plant-soil carbon belowground: a summary and synthesis. *Plant and Soil*,

187, 391–400.

Cao, M. K., D. P. Stephen, K. R. Li, B. Tao, J. Small, and X. Shao, 2003: Response of terrestrial carbon uptake to climate interannual variability in China. *Global Change Biology*, **9**, 536–546.

Cox, P. M., R. A. Betts, C. D. Jones, S. A. Spall, and I. J. Totterdell, 2000: Acceleration of global warming due to carbon-cycle feedbacks in a coupled climate model. *Nature*, **408**, 184–187.

Cramer, W., and Coauthors, 2001: Global response of terrestrial ecosystem structure and function to CO_2 and climate change: results from six dynamic global vegetation models. *Global Change Biology*, **7**(4), 357–373.

Dai, A., and I. Fung, 1993: Can climate variability contribute to the "missing" CO_2 sink? *Global Biogeochemical Cycles*, **7**, 599–609.

Dai, Y. J., and Coauthors, 2003: The common Land Model (CLM). *Bull. Amer. Meteor. Soc.*, **84**, 1013–1023.

Dan, L., J. J. Ji, and Y. P. Li, 2005: Climatic and biological simulations in a two-way coupled atmosphere-biosphere model (CABM). *Global and Planetary Change*, **47**, 153–169.

Fang, J. Y., G. H. Liu, and S. L. Xu, 1996a: Carbon cycle of terrestrial ecosystems in China and its global significance. *Hot Spots in Modern Ecology*, Wang et al., Eds., China Science and Technology Press, Beijing, 24–250. (in Chinese)

Fang, J. Y., G. H. Liu, and S. L. Xu, 1996b: Carbon pools in terrestrial ecosystems in China. *Hot Spots in Moden Ecology*, Wang et al., Eds., China Science and Technology Press, Beijing, 251–277. (in Chinese)

Fang, J. Y., S. L. Piao, J. S. He, and W. H. Ma, 2003: Increasing net primary production in China from 1982 to 1999. *Frontiers in Ecology and the Environment*, **1**(6), 293–297.

Foley, J. A., I. C. Prentice, N. Ramankutty, S. Levis, D. Pollard, S. Sitch, and A. Haxeltine, 1996: An integrated biosphere model of land surface processes, terrestrial carbon balance, and vegetation dynamics. *Global Change Biology*, **4**, 561–579.

Ge, Q., M. Zhao, and J. Zheng, 2000: Land use change of China during the 20th century. *Acta Geographica Sinica*, **55**(6), 698–706.

Grace, J., and Coauthors, 1995: Carbon dioxide uptake by undisturbed tropical forests in Southwest Amazonia, 1992 and 1993. *Science*, **270**, 778–780.

Hanson, P. J., and Coauthors, 2004: Oak forest carbon and water simulations: Model comparisons and evaluations against independent data. *Ecological Monographs*, **74**(3), 443–489.

Haxeltine, A., and I. C. Prentice, 1996: BIOME3: An equilibrium terrestrial biosphere model based on ecophysiological constraints, resource availability, and competition among plant functional types. *Global Biogeochemical Cycles*, **10**(4), 693–709.

Hou, H. Y., 1983: Vegetation map of China, 1:14000000. *Annals of the Missouri Botanical Garden*, **70**(3),

509–548.

Huang, M., 2005: The simulations of water, heat and carbon cycle in the ecosystem of continental China. Ph. D. dissertation, Institute of Geographic Sciences and Natural Resources Research, Chinese Academy of Sciences, Beijing, China, 137pp. (in Chinese)

IGBP Terrestrial Carbon Working Group, 1998: The terrestrial carbon cycle: implications for the Kyoto Protocol. *Science*, **280**, 1393–1394.

Kichlighter, D. W., and Coauthors, 1999: A first-order analysis of the potential role of the potential role of CO2 fertilization to affect the global carbon budget: a comparison of four terrestrial biosphere models. *Tellus*, **51B**, 343–366.

Kirschbaum, M. U. F., and Coauthors, 1994: Modelling forest response to increasing CO2 concentration under nutrient-limited conditions. *Plant, Cell and Environment*, **17**(10), 1081–1099.

Liu, H., W. Dong, C. Fu, and L. Shi, 2004: The long-term field exptEon aridification and the ordered human activity in semi-arid area at Tongyu, Northeast China. *Climatic and Environmental Research*, **9**(2), 378–389. (in Chinese)

Liu, J., H. Tian, M. Liu, D. Zhuang, J. Melillo, and Z. Zhang, 2005: China's changing landscape during the 1990s: Large-scale land transformation estimated with satellite data. *Geophys. Res. Lett.*, **32**, L02405, doi: 10.1029/2004GL021649.

Long, S. P., E. A. Ainsworth, A. D. B. Leakey, J. Nosberger, and D. R. Ort, 2006: Food for thought: lower-than-expected crop yield stimulation with rising CO_2 concentrations. *Science*, **312**(5782), 1918–1921.

Lü, A., H. Tian, M. Liu, J. Liu, and J. M. Melillo, 2006: Spatial and temporal patterns of carbon emissions from forest fires in China from 1950 to 2000. *J. Geophys. Res.*, **111**, D05313, doi: 10.1029/2005JD006198.

Luo, T. X., 1996: Patterns of biological production and its mathematical models for main forest types of China. Ph. D. dissertation, Committee of Synthesis Investigation of Natural Resources. Chinese Academy of Sciences, Beijing, China, 211pp. (in Chinese)

Mao, J. F., 2006: Improvements and applications of the Sheffield Dynamic Global Vegetation. Ph. D. dissertation, Institute of Atmospheric Physics, Chinese Academy of Sciences, Beijing, China, 149pp. (in Chinese)

Mao, J. F., B. Wang, Y. Dai, F. I. Woodward, P. J. Hanson, and M. K. Lomas, 2007: Improvements of a dynamic global vegetation model and simulations of carbon and water at an up-land oak forest. *Adv. Atmos. Phys.*, **24**(2), 311–322.

McGuire, A. D., and Coauthors, 2001: Carbon balance of the terrestrial biosphere in the twentieth century: Analyses of CO_2, climate and land use effects with four process-based ecosystem models. *Global Biogeochemical Cycles*, **15**, 183–206.

Melillo, J. M., I. Prentice, G. D. Farquhar, E. D. Schulze,

and O. E. Sala, 1996: Terrestrial biotic responses to environmental change and feedbacks to climate. *Climate Change: The Science of Climate Change*, Houghton et al., Eds., 1995, Cambridge University Press, Cambridge, UK, 444–481.

Mitchell, T. D., and P. D. Jones, 2005: An improved method of constructing a database of monthly climate observations and associated high-resolution grids. *International Journal of Climatology*, **25**(6), 693–712.

Ni, J., 2001: Carbon storage in terrestrial ecosystems of China: estimates at different spatial resolutions and their responses to climate change. *Climatic Change*, **49**, 339–358.

Ni, J., 2002: Effects of climate change on carbon storage in boreal forests of China: A local perspective. *Climatic Change*, **55**(1–2), 61–75.

Olson, R. J., J. M. O. Scurlock, S. D. Prince, D. L. Zheng, and K. R. Johnson, 2001a: NPP multi-biome: Global primary production data initiative products. The Oak Ridge National Laboratory Distributed Active Archive Center, Oak Ridge, Tennessee, US. [Available on-line from http://www.daac.ornl.gov/].

Parton, W. J., and Coauthors, 1993: Observations and modeling of biomass and soil organic matter dynamics for the grassland biome worldwide. *Global Biogeochemical Cycles*, **7**, 785–809.

Prentice, I. C., M. T. Sykes, and W. Cramer, 1993: A simulation model for the transient effects of climate change on forest landscapes. *Ecological Modelling*, **65**, 51–70.

Prince, S. D., R .J. Olson, G. Dedieu, G. Esser, and W. Cramer, 1995: Global primary production data initiative project description. IGBP-DIS Working Paper No. 12, International Geosphere-Biosphere Program-Data and Information System, Toulouse, 38pp.

Sellers, P. J., Y. Mintz, Y. C. Sud, and A. Dalcher, 1986: A simple biosphere model (SIB) for use within general circulation models. *J. Atmos. Sci.*, **43**, 505–531.

Shugart, H. H., 1998: *Terrestrial Ecosystems in Changing Environments*. Cambridge University Press, Cambridge, UK, 537pp.

Sitch, S., and Coauthors, 2003: Evaluation of ecosystem dynamics, plant geography and terrestrial carbon cycling in the LPJ dynamic global vegetation model. *Global Change Biology*, **9**, 161–185.

Tao, B., 2003: The simulations of the net primary productivity and net ecosystem productivity in the ecosystem of continental China. Ph. D. dissertation, Institute of Geographic Sciences and Natural Resources

Research, Chinese Academy of Sciences, Beijing, China, 157pp. (in Chinese)

Tian, H., J. M. Mellillo, D. W. Kicklighter, A. D. McGuire, and J. V. K. Helfrich, 1999: The sensitivity of terrestrial carbon storage to historical climate variability and atmospheric CO_2 in the United States. *Telles*, **51B**, 414–452.

Tian, H., J. M. Mellillo, D. W. Kicklighter, S. Pan, J. Liu, A. D. McGuire, and B. III. Moore, 2003: Regional carbon dynamics in monsoon Asia and its implications for the global carbon cycle. *Global and Planetary Change*, **37**, 201–217, doi: 10.1016/S0921-8181(02)00205-9.

Valentini, R., 2002: *Fluxes of Carbon, Water and Energy of European Forest.* Springer, Verlag, Heidelberg, 260pp.

Wang, Y. P., B. Z. Houlton, and C. B. Field, 2007: A model of biogeochemical cycles of carbon, nitrogen, and phosphorus including symbiotic nitrogen fixation and phosphatase production. *Global Biogeochemical Cycles*, **21**, GB1018, doi:10.1029/2006GB002797.

Woodward, F. I., 2002: Potential impacts of global elevated CO_2 concentrations on plants. *Current Opinion in Plant Biology*, **5**, 207–211.

Woodward, F. I., and M. R. Lomas, 2004: Vegetation dynamics—Simulation responses to climatic change. *Biological Reviews*, **79**, 643–670.

Woodward, F. I., T. M. Smith, and W. R. Emanuel, 1995: A global primary productivity and phytogeography model. *Global Biogeochemical Cycles*, **9**, 471–490.

Woodward, F. I., M. R. Lomas, and S. E. Lee, 2001: Predicting the future productivity and distribution of global terrestrial vegetation. *Terrestrial Global Productivity*, Roy et al., Eds., Academic Press, San Diego, USA, 521–541.

Xiao, X., J. M. Melillo, D. W. Kicklighter, Y. Pan, A. D. McGuire, and J. Helfrich, 1998: Primary production of terrestrial ecosystems in China and its equilibrium responses to changes in climate and atmospheric CO_2 concentration. *Acta Phytoecologica Sinica*, **22**, 97–118.

Yang, X., M. X. Wang, and Y. Huang, 2001: The climatic-induced net carbon sink by terrestrial biosphere over 1901–1995. *Adv. Atmos. Sci.*, **18**(6), 1192–1206.

Yu, Y., R. Yu, X. Zhang, and H. Liu, 2002: A flexible global coupled climate model. *Adv. Atmos. Sci.*, **19**, 169–190.

Zhou, G., and X. Zhang, 1996: Study on NPP of nature vegetation in China under climate change. *Acta Phytoecologica Sinica*, **20**, 11–19.